**Light Metals 2015**
*Edited by: Margaret Hyland*
***TMS (The Minerals, Metals & Materials Society), 2015***

# Frequency Response Analysis of Electrolysis Cell Voltage Signals during the Alumina Feed Cycles

Luísa Morais Azevedo
*Electrical Engineering Department*
*Federal University of Maranhão*
*São Luís, Brazil*
*luisamazevedo89@gmail.com*

Nilton Freixo Nagem
*Potroom Process Control*
*Aluminum Consortium of Maranhão - ALUMAR*
*São Luís, Brazil*
*nilton.nagem@alcoa.com*

João Viana da Fonseca Neto
*Electrical Engineering Department*
*Federal University of Maranhão*
*São Luís, Brazil*
*jviana@dee.ufma.br*

***Abstract*—Aiming a new view at pot feed cycles and to learn about the anode effect's peculiarities, the cell voltage was analyzed in the frequency domain through its power spectrums and the patterns were classified statistically at different stages of cell feeding. The results show that the power during the overfeed and underfedd remained at a low amplitude without drastic changes. A power increase was seen as the pots got closer to anode effect, even when, in the time domain, its behaviors were similar to normal operation. This analysis method fulfilled its purpose of providing both new information about the alumina feed cycles and a characteristic behavior near to the anode effect.**

***Keywords*-alumina feed cycles; anode effect; frequency domain; voltage;**

## I. Introduction

The alumina feed cycles are a routine activity in electrolytic aluminum production in smelters. In order to maintain the electrochemical process, shots of alumina are fed in varying periods of time [1]. One can estimate the effectiveness of the feed strategy by monitoring parameters that provide an indirect view of the process: resistance and voltage of the electrolysis cells. Although these parameters are useful in many situations, unusual events aren't easily detectable by them.

The parameters previously mentioned are analyzed in the time domain and, to identify any problems, their variations are studied. The cell voltage, for example, gives an overview of the electrochemical reaction: it is a sum of all the effects of the punctual reactions that occur at the same time inside the pot. Therefore this method isn't well suited to detect any punctual abnormality, such as anode effects, until it turns into a global event. A way to obtain a spatial view of the process is through the anode current measurements that demand costly devices that aren't available at the majority of the smelters around the world.

Recently, there have been some new approaches to the study of these signals. The restriction of the analyzes to the time response narrows their results even if the signal is the anode current. To overcome this limitation, studies applying the frequency response have been done and they present some outstanding results. The frequency response analysis of the anode current accomplished a further explanation to the influence of the bubbling process fluctuations during normal operation and during abnormal operation, for example when an anode has been misplaced [2]. A similar approach was replicated on cell voltage. However it hasn't been used to distinguish different states of operation but to superficially comprehend the process [9].

The possibilities opened by the work seen in [2] and [9] are a incentive to others in the frequency response analysis field. The alliance between the studies in time and frequency domains supply a range of new information that can not only improve the alumina feed strategies but also eliminate harmful events, e.g. anode effects [5]. The results of a tighter control are positive both environmentally and economically, considering that abnormal events lead to unnecessary waste of energy.

In this paper, the cells' voltage signals are analyzed in the frequency domain, rather than the normal time domain. First, we describe the way the voltage signals were sampled and processed. Then, the pairing between time and frequency domains by using the Fourier transform is explained. Next, the power spectrums are analyzed in order to see a visual pattern. After, a statistical analysis is done in a specific frequency range to better understand the behavior of the power spectrums in each situation. Finally, the results are discussed and the applicability of the technique in the real process is considered. The next steps and possible applications of the results are also discussed in this text.

## II. Methodology

First of all, the voltage signal is collected from the pots at the moments of interest. For example, at the beginning of overfeed. A filter must be applied to the signals in order to specifically study the voltage variation resulting from the events in focus.

After this pairing between time and frequency domains is done by applying the Fast Fourier Transform Algorithm. Finally, the power density spectrums obtained in the previous step, are studied both visually and statistically.

### A. Sampling Process

The sampling process was done by operating a software allowing implementation of triggers in a way that the users have the possibility to choose the beginning of their samples. This is an important characteristic considering the voltage signal won't be studied in all stages of the process, but only in few moments of the feed cycle and right before anode effects. The sampling period feasible with this software is 200 ms, i.e. a frequency of 5 Hz.

Some stages of the feed cycles were chosen to be sampled in order to obtain the differences among the alumina feed cycles and the neighborhood of the anode effect that are not evident in the time domain, justifying the analysis in the frequency domain. Knowing that near anode effect the voltage magnitude tends to rise, another situation in which this phenomenon also happens was chosen in order to compare the different power spectrums obtained from similar signals in the time domain.

The underfeed is the most important stage of the alumina feed strategy. In this step the amount of dissolved alumina in the electrolytic bath decreases with the time. This stage is fundamental to clean any extra concentration of alumina that was not consumed by the electrolysis before. It also helps to control the pot voltage to low levels. However, the relation between alumina concentration and the voltage isn't linear for any quantity of alumina [4].

Normally the voltage varies almost in a linear way with alumina concentration. It is known though that at lower alumina concentrations the voltage grows exponentially as the concentration of this oxide decreases. This kind of event is seen most of all at the end of the underfeed, when the concentration has decreased to limit levels. At this moment the signal was sampled.

Another stage of the feed cycle is overfeed, in which the concentration of alumina is increased with time in order to reverse its low levels obtained in the underfeed. However, the alumina doesn't dissolve right after it is added to the bath [4]. A delay between the increase of the feed rate and the real increase of alumina dissolved is observed at the beginning of the overfeed. Therefore, the behavior of the voltage when the overfeed starts resembles to the one seen at the end of the underfeed and near the anode effect.

In summary, signals with similar behaviors in the time domain were chosen as following: the approach of the anode effect, the end of underfeed and the beginning of overfeed. The similarity among them can be seen below (Figure 1).

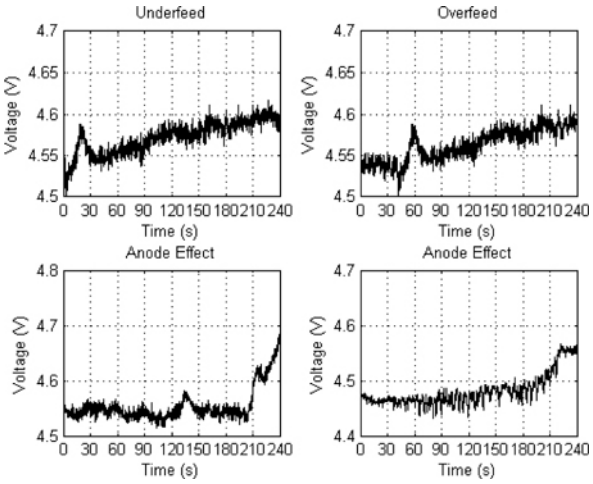


Figure 1. Comparing Underfeed, Overfeed and Anode Effect Time Responses.

### B. Windowing Process

The samples obtained in the preceding step correspond to four minutes data blocks. In order to study the signal in shorter periods of time, a technique called windowing was applied. Another reason to do this is because the signal is sampled during a finite time, leading to data that correspond to fractions of the original signal's period. Because of the incomplete periods, the sampled signal will represent a truncated wave form of the original signal.

The windowing process allows to divide the data blocks, to define a complete period inside the window and to mitigate problems due to discontinuity [3]. Thus this technique improves the spectral characteristics of the signal, which is fundamental to the next step.

This process consists basically in the convolution in the frequency domain of the signal to be windowed and a function that will be called window. In this case, multiplication of the sampled signal with a kind of window called Hamming, determined by the following equation (1).

$$w[n] = 0.54 - 0.46 \times \cos\left(\frac{2\pi}{n}\right), n = 0, 1, 2...N-1 \quad (1)$$

Where $N$ is the size of the window. In this context, with a sampling frequency of 5 Hz, each data block has 1200 data points. The blocks were divided by using the windowing technique into blocks of one minute, i.e. 300 data points, which corresponds to the size of the window, $N$.

The one minute window was slid all along the four minute block, and the result of their multiplication in time was done every thirty seconds. In other words, blocks of one minute results of the windowing process were stocked in an interval of thirty seconds between them. This can be visualized in Figure 2.

Associated to the windowing process, detrending of this signal was done. The reason to do so is to analyze only the variations that occurs in the limited time inside the window. This also helps to overcome the discontinuity problem cited before [10]. Another procedure done in this stage was the normalization of the vectors corresponding the data of each cell at each moment.

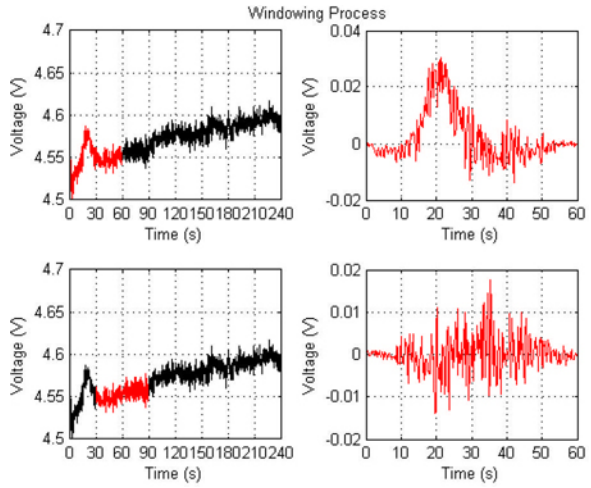


Figure 2. Windowing Process.

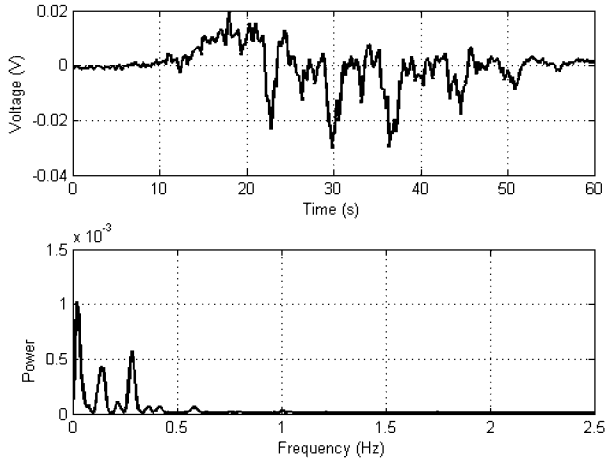


Figure 3. Cell Voltage Time Response (above) and Frequency Response (below).

### C. Fast Fourier Transform

The one minute data blocks being in the time domain, Fast Fourier Transform was applied to obtain the frequency response. Thereby, the cell voltage signal time response turned out to frequency response, resulting in a signal which represents power ($V^2/Hz$) in function of frequency ($Hz$) [7].

This way of presenting the frequency response is known as the power density spectrum (PDS) [7]. Fast Fourier Transform was applied every thirty second in a one minute window as shown in Figure 3.

### D. Random Process, a Statistical Overview

The windows' power density associated to each frequency characterize a kind of process. This process represents the variation of the power in each frequency as the time goes by. The spectrum's analysis as done by Bao [2] is narrowed to visual conclusions. In this paper, a numerical way to show the properties of this process was perfomed.

The process of power density versus time was characterized in a statistical way. Properties as stationarity, variance and mean were calculated for each event (underfeed, overfeed and anode effect) [6] [8]. Therefore it was possible to distinguish in a better way the frequency response of the events at the chosen moments.

The number of event characterization adopted in this paper were ten for underfeed and overfeed,and three anode effects. Four pots were studied. A total of forty data blocks of underfeed and overfeed were stored and twelve anode effects.

## III. Results and Discussion

The results were analyzed at each interest point in the alumina feed cycle. First, examples of the frequency response at some stages of the alumina feed process and in the neighborhood of the anode effect were displayed. It's worth mentioning that these power spectrums do not represent a standard behavior of the analyzed pots. Next, the statistics of each stage of the process studied were displayed, this time a normal behavior for each event analyzed.

### A. Power Spectrums

*1) Overfeed Power Spectrums:* In order to illustrate the kind of signal obtained at the frequency domain, the overfeed signal showed in Figure 1 was taken as an example. By using the windowing process and the Fourier transform, the representation was acquired as seen in Figure 4. The biggest power amplitude is found at lower frequencies. Specifically at 0.02 Hz frequency, where the largest variations are noticed. As the overfeed moves away from its beginning, the power at this specific frequency increases. However, this kind of behavior is not replicated to all the characterization done at the beginning of the overfeed.

In detail, Figure 5 displays the PDS for each window. The frequency range on the x-axis was chosen in a way that specifically highlights the variations at 0.02 Hz. The frequency at this point behaves in a oscillatory way as overfeed progresses. The maximum power is obtained at the fourth minute of overfeed. However, as stated before, this is not a standard behavior for all pots and for all overfeeds.

*2) Underfeed Power Spectrums:* The results for the underfeed are shown in the same way as for overfeed. The underfeed data presented in Figure 1 is displayed in the frequency domain in Figure 6. One can see, particularly at 0.02 Hz, that power decreases as underfeed draws to a close. Nevertheless, this proceeding isn't repeated in the other 39 underfeed characterizations explored in this work. Such divergent results led the statistical analysis to be necessary. Analyzing Figure 7, the power at 0.02 Hz on the last minute decreases drastically.

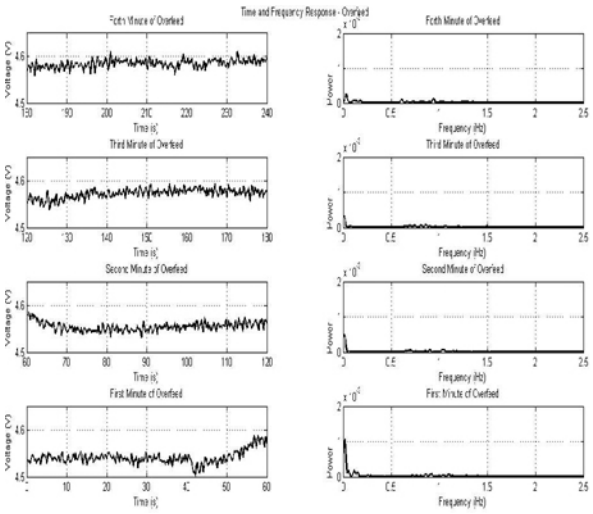

Figure 4. Time and Frequency Response at the Overfeed.

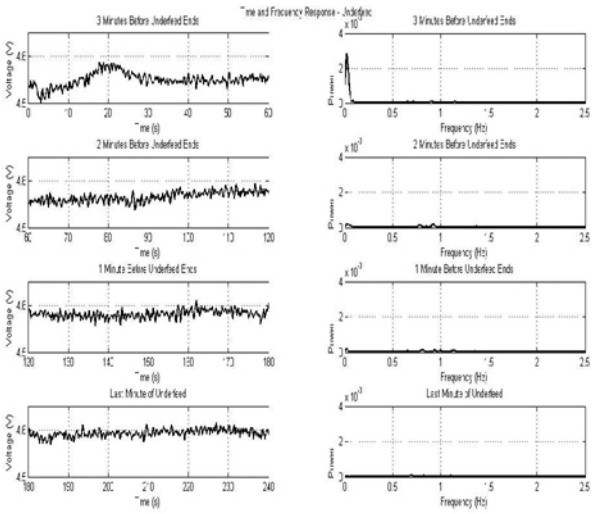

Figure 6. Time and Frequency Response at the Underfeed.

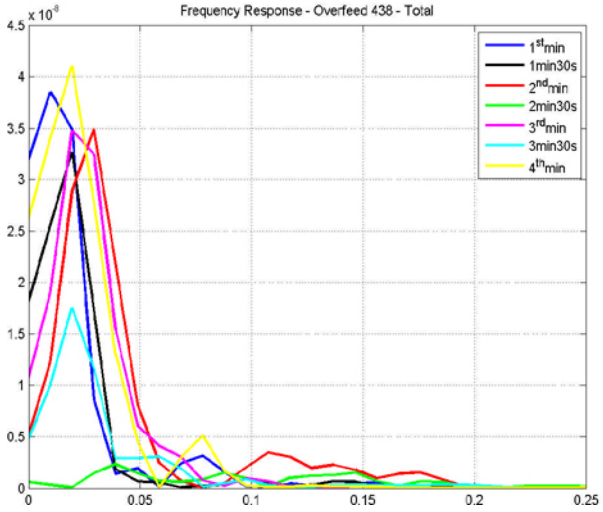


Figure 5. Frequency Response at the Overfeed in Detail.

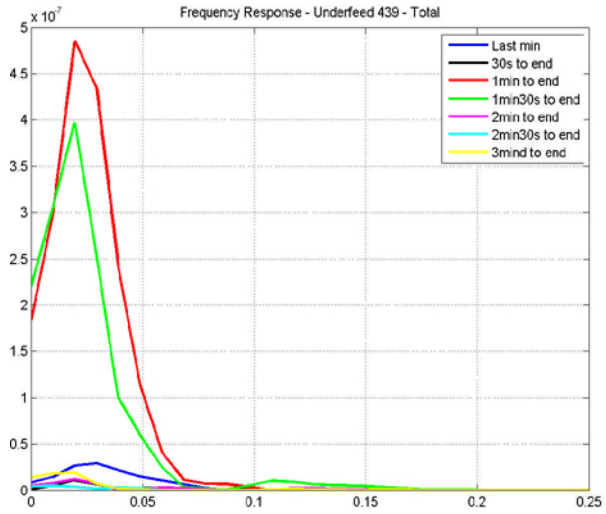


Figure 7. Frequency Response at the Underfeed in Detail.

*3) Anode Effect Power Spectrums:* Finally, the anode effect power spectrums of the signal stated in Figure 1 are shown in Figure 8. Observing the 0.02 Hz power, an increase is seen as the anode effect aproaches. This behavior doesn't recur in the other characterization though. However, the power is very small 30 seconds before anode effect begins(black line in Figure 9). This power "jump" is not seen on the other anode effects studied. The lack of information obtained from the visual tests for all the events studied has led to the statistical characterization presented in the next section.

### *B. Characterization of the Processes*

As the power at 0.02 Hz frequency revealed a random behavior between all the cases studied, statistical characterization of this fluctuation was necessary. The statistical moments of first and second order were analyzed (Tables I, II and III) and the results are presented in Figure 10 as boxplots.

One can see from tables I, II and III the mean on the neighborhood of the anode effect is about one order of magnitude greater than in the overfeed and underfeed in some moments. Another characteristic is the larger dispersion of the power values presented nearby the anode effect, this can

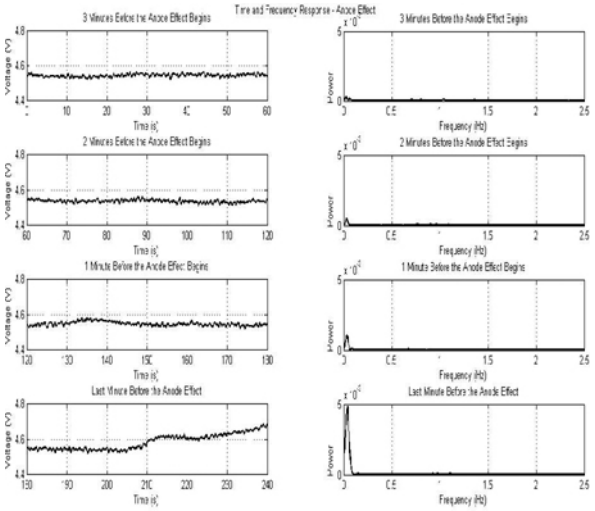

Figure 8. Time and Frequency Response Before the Anode Effect.

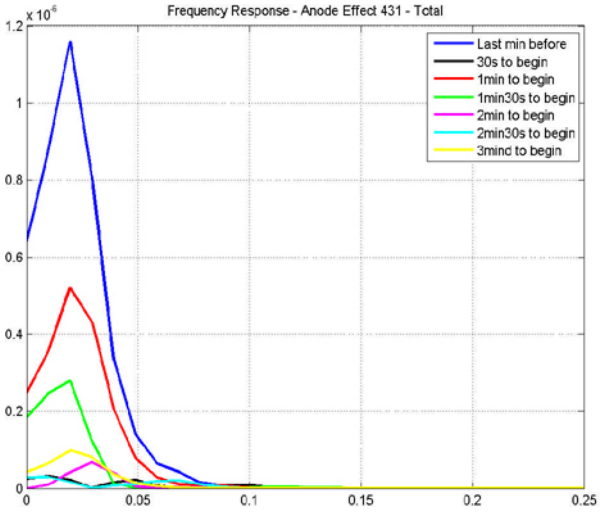


Figure 9. Frequency Response Before the Anode Effect in Detail.

be seen analyzing the variance.

This dispersion can be seen also in the boxplot (Figure 10) where the box corresponding to the anode effect data is larger than the others. Another important attribute of this event can be noticed especially three minutes before its beginning, when nearly all the power data obtained next to anode effect is superior than the others. In other moments, the distinct values belonging to the characteristic of before anode effect corresponds to half of the values collected for this event. This observation confirms what was noticed from the means values on the tables, leading to the conclusion the power at this frequency is enlarged as the cell approaches

Table I
MEAN AND VARIANCE OF THE SPECTRAL POWER DURING THE OVERFEED.

| Moment | Mean $(V^2/Hz)$ | Variance $(V^2/Hz)^2$ |
|---|---|---|
| $4^{th}$min | $6.26 * 10^{-8}$ | $2.38 * 10^{-14}$ |
| 3min30s | $4.65 * 10^{-8}$ | $1.46 * 10^{-14}$ |
| $3^{rd}$min | $4.21 * 10^{-8}$ | $4.89 * 10^{-15}$ |
| 2min30s | $5.98 * 10^{-8}$ | $2.51 * 10^{-14}$ |
| $2^{nd}$min | $7.53 * 10^{-8}$ | $8.44 * 10^{-14}$ |
| 1min30s | $3.46 * 10^{-8}$ | $4.83 * 10^{-15}$ |
| $1^{st}$min | $5.08 * 10^{-8}$ | $9.77 * 10^{-15}$ |

Table II
MEAN AND VARIANCE OF THE SPECTRAL POWER DURING THE UNDERFEED.

| Moment | Mean $(V^2/Hz)$ | Variance $(V^2/Hz)^2$ |
|---|---|---|
| 3min to end | $8.24 * 10^{-8}$ | $3.07 * 10^{-14}$ |
| 2min30s to end | $6.22 * 10^{-8}$ | $1.18 * 10^{-14}$ |
| 2min to end | $8.11 * 10^{-8}$ | $2.30 * 10^{-14}$ |
| 1min30s to end | $7.33 * 10^{-8}$ | $1.76 * 10^{-14}$ |
| 1min to end | $5.54 * 10^{-8}$ | $3.45 * 10^{-14}$ |
| 30s to end | $1.96 * 10^{-8}$ | $1.50 * 10^{-15}$ |
| Last minute | $4.53 * 10^{-8}$ | $1.23 * 10^{-14}$ |

to the anode effect.

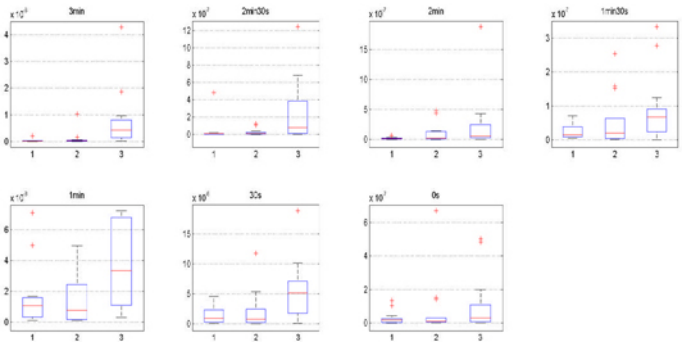

Figure 10. BoxPlot comparing 1 - Overfeed, 2 - Underfeed and 3 - Anode Effect.

## IV. CONCLUSION

The results' analysis showed that from three to two minutes before the anode effect, the power on the studied range is larger than in overfeed and underfeed. This power is also decreased as the anode effect event approaches, behaving similarly to the cell in normal operation. Differences between the alumina feed stages were not observed by the analysis done in this paper.

The results which distinguish anode effect from normal operation are interesting as they may enable predicting and avoiding the occurrence of this kind of event. The prediction could be done through the implementation of triggers. These triggers would fire whenever the power exceeded a certain threshold flagging a possible occurrence of anode effect. As

Table III
MEAN AND VARIANCE OF THE SPECTRAL POWER BEFORE THE ANODE EFFECT.

| Moment | Mean $(V^2/Hz)$ | Variance $(V^2/Hz)^2$ |
|---|---|---|
| 3min to begin | $7.83 * 10^{-7}$ | $1.25 * 10^{-12}$ |
| 2min30s to begin | $2.69 * 10^{-7}$ | $1.36 * 10^{-13}$ |
| 2min to begin | $2.46 * 10^{-7}$ | $2.39 * 10^{-13}$ |
| 1min30s to begin | $8.98 * 10^{-8}$ | $9.84 * 10^{-15}$ |
| 1min to begin | $3.82 * 10^{-8}$ | $1.13 * 10^{-16}$ |
| 30s to begin | $5.37 * 10^{-8}$ | $2.41 * 10^{-15}$ |
| Last minute | $1.10 * 10^{-7}$ | $2.91 * 10^{-14}$ |

the power is increased approximately three minutes before anode effect, there would be enough time to enable anode effect's suppression routines.

This is an important opportunity to reduce emissions of pollutant gases from the electrolysis process, preserving the environment. For future works, statistical characterization of anode current signals in frequency domain could be performed. Another form could be to extend the knowledge obtained on this article by applying techniques of pattern recognition, neural networks or even fuzzy systems and cluster algorithms. The characterization of these events associating features in time and frequency can result in new knowledge and anode effect prediction tools.

## ACKNOWLEDGMENT

The authors would like to thank to the Aluminium Consortium of Maranhão (ALUMAR) for providing their facilities for the development of this work and relevant data from their process. For the same reason, thanks to the Federal University of Maranhão, CAPES Foundation (Coordination of Improvement of Higher Education Personnel) and PPGEE (Graduate Program in Electrical Engineering).

## REFERENCES

[1] *QLC User's Manual, Alcoa Internation Document.*

[2] J. Bao M. Skyllas-Kazacos B. J. Welch C. Cheung, C. Menictas. Frequency response analysis of anode current signals as a diagnostic aid for detecting approaching anode effects in aluminum smelting cells. 2013.

[3] Barrie W. Jervis Emmanuel C. Ifeachor. *Digital Signal Processing, A Pratical Approach.* Addison Wesley Publishing Company, 1993.

[4] Kuawde H. Grotheim, K. Understandig the hall heroult process for production of aluminum. Dusseldorf Aluminum Verlag, 1986.

[5] Serger E.J. Haupin, W. Aiming for zero anode effects. *The Minerals, Metals and Materials Society*, 2001.

[6] Krusche N. Piccoli H. C. Pinto, E. L. C. Análise estatística e espectral de dados meteorológicos de superfície. 1996.

[7] Barry Van Veen Simon S. Haykin. *Sinals and Systems.* 1999.

[8] M.R. Spiegel. *Probabilidade e Estatística.* 1978.

[9] Jayson Tessier. Estimation of pseudoresistance power density spectrum at mt-holly. Live Meeting, 2013.

[10] Yi S. H. Yoo, C. S. Effects of detrending for analysis of heart rate variability and applications to the estimation of depth of anesthesia. *Journal of the Korean Physical Society*, 44(3), October 2003.